HHS Public Access

Author manuscript

Adv Healthc Mater. Author manuscript; available in PMC 2020 October 01.

Published in final edited form as:

Adv Healthc Mater. 2019 October ; 8(19): e1900558. doi:10.1002/adhm.201900558.

A Critical Review of Microelectrode Arrays and Strategies for Improving the Neural Interface

Morgan Ferguson, **Dhavan Sharma**, **David Ross**, **Feng Zhao***

Department of Biomedical Engineering, Michigan Technological University, 1400 Townsend Dr., Houghton, MI 49931

Abstract

Though neural interface systems (NISs) could provide a potential solution for mitigating the effects of limb loss and central nervous system (CNS) damage, the microelectrode array (MEA) component of NISs remains a significant limiting factor to their widespread clinical applications. Several strategies can be applied to MEA designs to increase their biocompatibility. Herein, we have provided an overview of NISs and their applications, along with a detailed discussion of strategies for alleviating the foreign body response (FBR) and abnormalities seen at the interface of MEAs and the brain tissue following MEA implantation. Various surface modifications, including natural/synthetic surface coatings, hydrogels and topography alterations, have shown to be highly successful in improving neural cell adhesion, reducing gliosis, and increasing MEA longevity. Different MEA surface geometries, such as those seen in the Utah and Michigan arrays, can help alleviate the resultant FBR by reducing insertion damage, while providing new avenues for improving MEA recording performance and resolution. Increasing overall flexibility of MEAs as well as reducing their stiffness have also been shown to reduce MEA induced micromotion along with FBR severity. By combining multiple different properties into a single MEA, the severity and duration of an FBR post-implantation could be reduced substantially.

Graphical Abstract

This paper provides an overview of neural interface systems and their applications, along with a detailed discussion of strategies for alleviating the foreign body response and abnormalities seen at the interface of microelectrode array (MEA) and the brain tissue following the MEA implantation.

***Corresponding to:** Feng Zhao, Department of Biomedical Engineering, Michigan Technological University, 1400 Townsend Drive, Houghton, MI 49931, U.S., Tel: 906-487-2852, Fax: 906-487-1717, fengzhao@mtu.edu.

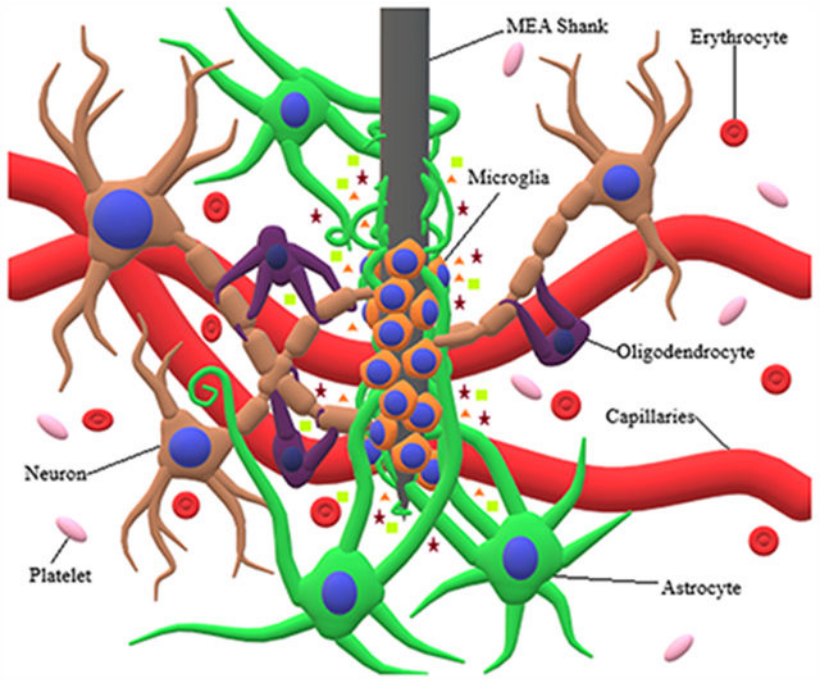

Keywords

Microelectrode array; foreign body response; surface modification; stiffness

1. Introduction

The human brain is of paramount importance to human survival, as it controls almost every physiological action characteristic of the body, including movement, maintenance of homeostasis, sensation, and various other functions. As such, the onset of neurological complications can be lifechanging, making performance of daily tasks extremely difficult, or even rendering an individual completely incapable of conducting normal daily operations. One such neurological complication is spinal cord injury (SCI), which can cause someone to become partially or completely paralyzed. Every year, there are approximately 17,000 new cases of spinal cord injury in the United States [1]. Moreover, other neurological complications including strokes and neurodegenerative disorders such as amyotrophic lateral sclerosis (ALS) make life challenging [2]. Another common injury that may not be directly related to complications of the nervous system, but still has significant impact on an individual's life, is limb loss. It is estimated that 185,000 people in the United States undergo amputation procedures every year, with a total of approximately 2 million people suffering from limb loss in the United States alone. By 2050, the amount of people living with limb loss in the United States is expected to increase to 3.6 million [3]. At present time, there is no cure for the previously mentioned conditions.

However, while complete restoration of the neurological system may be a long-term goal, improving such conditions may be possible using neural interface systems (NISs). Typically, NISs involve establishing connection between the brain and an external apparatus by

surgically implanting a microelectrode array (MEA) into the brain. Generally, NISs are composed of four components, including an MEA, an output device, a mapping or decoding algorithm, and sensory feedback [2]. Regardless of the intended application or the complexity of a NIS, though, an MEA must be present in the brain for a NIS to work. Despite the fact that NISs have enormous potential for treating neurological complications, several issues with MEAs prevent NISs from being clinically applicable on a large scale. One of them is their substantial mechanical differences to those of tissues and cells of the brain.

For the past few decades, MEAs have been fabricated using silicon, glass, and metal (tungsten) microtechnologies [4]. The overall stiffness of these materials is characterized by a Young's modulus in the range of GPa. Silicon, for instance, possesses a Young's modulus of approximately 190 GPa [5]. Glass, depending on chemical composition, can have a Young's modulus between 60 and 100 GPa [6]. A metallic substance, such as tungsten, has a Young's modulus value of 410 GPa [7]. When observing tissues of the human body, the resulting Young's modulus is significantly lower, within the range of kPa, according to indentation tests. In fact, tissues of the brain are extremely soft and compliant, such as gray matter, possessing a Young's modulus of approximately 3 kPa [8], which is on a range of 2×10^7 to 1.37×10^8 times lower in stiffness than that of the aforementioned materials used to fabricate MEAs. Such a large mechanical difference between the MEA and brain is highly detrimental to both the brain and MEA itself. Other factors, such as cell adhesion to MEAs and initial insertion damage play a role as well. Without proper cell adhesion, the MEA will be free to move around inside the brain, causing additional stress on tissue that is already damaged by insertion of the MEA. In addition, proper cell adhesion is necessary for cell proliferation and healing to occur. The significantly higher stiffness of MEA materials contributes to poor cell adhesion and proliferation. Combined, all of the previously mentioned MEA properties reduce the biocompatibility of MEAs and cause the elicitation of a foreign body response (FBR). In this review, the response of brain cells to the presence of MEAs and how the resulting FBR affects both the brain and MEA itself is discussed. Moreover, novel MEA technologies and their effectiveness in improving both the neural interface and MEA performance is reviewed, specifically those strategies involving modifications to surface properties, mechanical properties, and geometry of MEAs.

2. Brain Foreign Body Response

Prior to discussing the long-term consequences of implanted MEAs in the brain, it is first important to understand how the brain initially responds to the presence of an implanted device. Usually, an FBR is characterized by various stages, including injury upon implantation, interactions between the device/biomaterial and surrounding tissue, acute inflammation, chronic inflammation, development of granulated tissue, and enclosure of the device/biomaterial in a fibrous capsule [9]. Such is the typical process for most of the human body. However, when dealing with the brain, it is necessary to take a different approach, as the brain does not use the exact same mechanisms or cells for removing a foreign body. The following sections will provide a brief discussion of these unique features.

2.1. Cell Types Present in the Brain

Due to the presence of the blood-brain barrier (BBB), many cell types, especially immune cells that are commonly found throughout the human body, are not present within the brain. To accommodate the presence of the BBB, the brain has developed its own repertoire of cells. There are two different general types of cells present in the brain: neurons and glial cells. Both neurons and glial cells share a common origin, arising during embryonic development from precursor cells of the neuroectodermal germ layer [10], which allows them to remain in the brain following BBB development.

Neurons are one of the most predominant cells in the nervous system that maintain overall brain function. They can be divided into three different sub-groups according to their function: (1) sensory neurons, (2) motor neurons, (3) and interneurons. Sensory neurons convey neural signals towards the central nervous system (CNS), and motor neurons convey neural signals away from the CNS, while interneurons conduct signals between the two [11]. It is commonly assumed that there are ten times more glial cells within the brain compared to that of neurons [12]. However, contrary to popular belief, it has been shown that the human brain is composed of similar amounts of both neurons (~86.1 ± 8.1 billion) and glial cells (~84.6 ± 9.6 billion) [13]. Along with neurons, glial cells play critical roles in the brain, including structural support and the local immune response. However, unlike neurons, they do not directly participate in electrical signal propagation or synaptic interaction [14]. There are various types of glial cells, including microglia, astrocytes, oligodendrocytes, and ependymal cells [11, 14–15].

Microglia compose about 12% of total brain cell mass and are characterized by their dark, elongated nucleus and limited cytoplasm; they are the smallest of all glial cells [11, 16]. Referred to as antigen presenting cells (APCs) due to their marked phagocytic activity and characteristic expression of major histocompatibility complex (MHC) class II antigens [17], microglia are the brain's equivalent to monocytes of the body's innate immune system and act as cytotoxic cells to protect the brain against infection [18]. Depending on the region of the brain, the overall density of resident microglia varies from 0.5 to 16.6% [19], with gray matter, along with regions of the olfactory telencephalon, hippocampus, basal ganglia, and substantia nigra, possessing the highest microglial concentrations [20].

Astrocytes are the most abundant type of glial cell, although the exact proportion of astrocytes in the brain is unclear. Studies have indicated, depending on the applied quantification technique, that astrocytes compose between 20-40% of all glial cells in the CNS [21]. They are large cells, possessing various extensions that give astrocytes a star-shaped appearance [11]. These extensions allow astrocytes to maintain connections with each other as well as with neurons and blood vessels, to effectively maintain the BBB's integrity [22]. Astrocytes can be further divided into three sub-groups based on their morphology and location, including radial astrocytes (ventricular system), protoplasmic astrocytes (gray matter) and fibrous astrocytes (white matter) [23]. They are responsible for a variety of functions including maintenance of brain homeostasis, neuromodulation, neuronal metabolic support, glial scar formation, and regulation of the CNS immune response [11, 24].

Oligodendrocytes are comparatively smaller cells characterized by both a dark nucleus and cytoplasm and are the most abundant type of glial cell in white matter. They are mainly responsible for secreting myelin, which ultimately wraps around axons of the brain, acting as an insulator to increase neuronal signaling speed [11, 25]. Ependymal cells are characterized by a cuboidal to columnar shape and are responsible for the secretion of cerebrospinal fluid (CSF), within which the brain is suspended [11, 26]. While all neural cells contribute to the brain FBR, the main players are microglia and astrocytes.

2.2. Initial Damage, Foreign Body Response, and Glial Scaring

Initial insertion of MEAs into the brain is a violent process that causes significant damage to the surrounding tissue. MEA insertion disrupts the BBB and damages capillaries, extracellular matrix (ECM), and neurons as well as glial cell functions. This mechanical trauma subsequently initiates the healing process, which shares distinct similarities to the healing of other body components. Additionally, the resulting trauma releases erythrocytes, activates platelets, and initiates the complement cascade. This ultimately results in cytokine secretion, which causes microglia and astrocytes to undergo significant changes [27].

The process involving participation of microglia and astrocytes in the brain FBR is known as reactive gliosis [28]. Under normal circumstances, microglia exist in a resting or ramified state, rather than a completely inactive state, and constantly monitor the brain environment for any abnormalities. However, under stimulation, microglia undergo significant changes from a ramified to ameboid morphology, allowing them to migrate to the site of injury or infection [29]. Additionally, microglia experience increased levels of proliferation [17] and begin secreting various chemokine attractants (i.e. RANTES/CCL5, monocyte chemoattractant protein (MCP)-1/CCL2, interferon γ, inducible protein (IP)-10/CXCL10, macrophage inflammatory protein (MIP)-1α/CCL3, MIP-1β/CCL4, and MIP-2/CXCL2) and proinflammatory cytokines (i.e. tumor necrosis factor (TNF)-α, brain derived neurotropic factor (BDNF), nerve growth factor (NGF), neurotrophin-3 (NF-3), various interleukins (IL), interferons (IFN), colony stimulating factors (CSF), and transforming growth factors (TFG)) [30]. It has been shown that upon MEA insertion, microglia extend processes, or lamellipodia, towards the implant surface. Within 30 minutes after MEA insertion, microglial lamellipodia begin to encapsulate the implant [31]. Approximately 12 hours following implantation, microglia can transition fully into their motile phase and begin moving towards the implanted MEA [32]. After 24 hours, the MEA can be surrounded by activated microglia that ultimately form an encapsulating sheath around the implant (Figure 1) [33].

Upon initiation of the brain FBR, astrocytes undergo transition from a normal to reactive phenotype, which is characterized by increased proliferation, ECM production, and migration [34]. Depending on the severity of FBR, reactive astrocytes may be characterized by mild to moderate astrogliosis, severe diffuse reactive astrogliosis, or severe reactive astrogliosis with glial scaring. In mild to moderate astrogliosis, relatively less proliferation of astrocytes is observed compared to severe astrogliosis, and is usually associated with mild brain trauma, viral and bacterial infections, or small brain lesions [35]. However, in severe diffuse reactive astrogliosis, astrocyte proliferation increases substantially, and hypertrophy

of astrocyte processes experiences a pronounced increase, which is normally seen when there is a large focal lesion [35].

If the FBR is severe enough, both severe reactive gliosis and glial scaring can occur. This is characterized by substantial proliferation of reactive astrocytes, which surround the site of injury and activated microglia through overlapping of large numbers of astrocytic processes (Figure 1) [35]. A dense encapsulating sheath or glial scar forms and ultimately results in substantial tissue reorganization and structural changes which last for an indefinite period [34b, 35–36]. This is typically what would be seen due to the presence of an MEA implant or the result of severe trauma, penetrative wounds, or chronic neurodegeneration [48]. Astrocytic encapsulation of an MEA has been shown to occur approximately 2-3 weeks following initial implantation [36–37]. However, glial scaring is not necessarily negative for brain tissue and cells. The previously mentioned changes resulting from glial scaring include substantial invasion of the lesion scar by epithelial cells for the reorganization of blood vessels and revascularization of the area surrounding the lesion scar [38]. Also, an inflammatory response is essential to promote healing of the damaged tissues [39]. Nevertheless, persistent FBR can be quite detrimental to the brain.

3. Biocompatibility and Performance Assessment of Microelectrode Arrays

MEA biocompatibility is a significant issue, which prevents their large-scale application in NISs. As aforementioned, MEAs are primarily fabricated using stiff, inorganic materials, with silicon arguably being the most popular. However, mechanical properties and surface topography are not the sole determinants of FBR severity. Ultimately, the severity and duration of an FBR depends on various factors including composition, contact duration, surface topography, and surface chemistry of the MEAs [9d]. Furthermore, the amount of damage caused by initial MEA insertion has significant impact on how the resulting FBR will proceed.

Initial MEA insertion damages the BBB, disrupts brain homeostasis, and causes dysfunction of CNS components [40]. Also, MEAs used in neural prosthetics are meant to remain within the brain for long periods of time. With current MEA technology, long-term implantation of MEAs in the brain can have a multitude of unfavorable consequences, for both the brain and MEA itself. Brain FBR can be quite detrimental if it persists for long periods of time, which stems from prolonged activation of microglia [16–18]. Another issue arises from the physical and chemical differences between MEAs and the brain. Because of those differences, proper cell adhesion becomes difficult, which results in MEA micromotion and increased strain on brain cells and tissues [41]. Also, combining MEA induced strain with the FBR in the brain, this ultimately causes normal MEA function to be compromised, either partially or completely [42].

3.1. Microelectrode Array Insertion

When an MEA is inserted in the brain, a significant amount of initial damage is caused to the BBB's neurovascular unit. The BBB is crucial for maintaining homeostasis in the CNS,

enclosing it in a protective vascular structure and effectively isolating the CNS from external blood circulation [43]. Upon disruption of the BBB, however, inflammation and microglial activation occurs, along with mitochondrial dysfunction and increased oxidative stress [44]. As such, damage to the BBB can have severe consequences. Bennett *et al.* [45] assessed BBB disruption caused by stab wounds and implantation of Utah MEAs, along with the overall consequences. Both stab wound and implantation groups saw upregulation of proinflammatory genes along with downregulation of genes for both tight junction (TJ) and adherens junction (AJ) proteins; this is suggestive of BBB dysfunction. In a separate study, Bennet *et al.* [40] also showed an interesting phenomenon regarding BBB disruption by MEAs. Upon BBB disruption, free iron is released into the parenchyma of the brain, which can further exacerbate the FBR through oxidative stress via Fenton chemistry. Iron plays a fundamental role in Fenton reactions, which produce reactive oxygen species (ROS). MEA induced injuries, if not rectified, can cause chronic micro-bleeding, iron overload, sustained ROS production, and further damage to the surrounding neural tissue [46].

Further adding to the damage caused by MEA insertion and BBB dysfunction is chronic activation of microglia. Microglia, as mentioned previously, are one of two main players in the overall brain FBR, which also includes astrocytes. While they are important for protection against infection or foreign materials, microglia can become neurotoxic if they remain active for long periods of time [47]. This is mainly due to their tendency to release ROS, nitric oxide (NO), and various proinflammatory factors such as TNF-α [30]. As such, they can potentially cause irreversible damage to the neurons and ECM of the surrounding tissue. Biran *et al.* [48] have demonstrated gliosis neurotoxicity by comparing overall damage to brain tissue over time between implanted MEAs and stab wounds in rats. A significant reduction in neuronal density was shown to occur around the MEAs in comparison to the stab wounds, which showed minimal neurofilament loss over time in comparison and eventual full neurofilament restoration.

3.2. Microelectrode Array Physical and Chemical Properties

One of the main problems with MEAs is that they are primarily fabricated using materials with substantial physical and chemical differences to that of brain tissues and cells. Normally, cells of both the brain and other soft tissues of the human body are accustomed to attaching to much softer surfaces with stiffness moduli on the order of 3-200 kPa [49]. This is cell type dependent, given that some cells, such as osteocytes, prefer to attach on stiffer surfaces [50], whereas neuronal cells have difficulty in attaching on stiffer surfaces. Additionally, topographical features on the substrate play a significant role in mediating cell attachment. However, lack of appropriate topographical features on the substrate could reduce focal adhesions [50], making it difficult for cells to proliferate, as they require stable adhesion in order to proliferate, which could become a problem during the healing phase after the MEA implantation.

Poor cell adhesion can result in MEA micromotion, which imposes additional strain on the brain [41b], causing exacerbated damage. Karumbaiah *et al.* [41a] demonstrated this occurrence, where astrocytes, microglia, and cortical neurons, were subjected to micromotion simulated stretch for set periods (4-23 hours for astrocytes, 2-12 hours for

microglia, and 2-8 hours for cortical neurons). It was discovered that over time, all cells experienced reduction in cell viability resulting from the applied strain, with cortical neurons experiencing the most pronounced drop in viability. Using stiff materials such as silicon and glass in MEA design adds risks to MEA micromotion and subsequent damages. Therefore, in moving forward with new MEA designs, it would be prudent to select mechanically compatible materials to the brain tissue. Also, it is possible to increase the amount of strain on the brain even further and exacerbate the FBR by tethering MEAs to the skull (Figure 2A). In another study [51], it was demonstrated that tethering MEAs to the skull caused additional strain on the surrounding brain tissues with a far more significant FBR than the control, in which the MEA was not tethered to the skull. As such, tethered MEA designs introduce a significant amount of risk to the patient and MEA itself, making them unsuitable for widespread clinical use.

Additional factors regarding the MEA, such as surface topography and electrode thickness, also have a significant influence on overall MEA induced strain and subsequent damage to brain tissues and cells. Yin *et al.* [52] applied kinetic analysis to MEAs for the expressed purpose of determining optimal parameters in MEA design, specifically tip fillet, wedge angle, electrode thickness, stiffness and surface friction coefficient. It was observed that MEAs with a tip fillet radius of 20 mm, wedge angle of 45°, thickness of 40 μm, Young's modus of 200 GPa, and frictional coefficient of 0.1 exhibited optimal performance. In a similar study, Ma *et al.* [53] used finite element (FE) models to test optimal MEA design parameters. Results showed that an MEA with a tip fillet of 20 μm, wedge angle of 70°, and wall thickness of 15 μm caused minimal injury from micromotion induced strain. Though the optimal values obtained for MEA parameters from the previously mentioned studies were different to some extent, this shows that proper MEA design is paramount for reducing micromotion and subsequent damage from MEA induced strain and the resultant FBR.

3.3. Microelectrode Array Performance

Aside from damage to the brain, there are also issues when it comes to the MEA itself after long-term implantation in the brain. Over time, MEAs experience a reduction in recording performance following prolonged FBR and MEA induced strain. In a study performed by Nolta *et al.* [42], 4×4 Utah Electrode Arrays were implanted into the cerebral cortex of young adult rats. The rats were monitored for device failure by determining the amount of recordable signal activity of each MEA. It was found that over a course of 12 weeks, there was an increase in recording failure among the MEAs. Similar phenomena were observed in a study by Debnath *et al.* [54], where MEAs were implanted into marmoset brains and monitored for signal stability and quality over the course of several months. Over time, many of the MEAs lost signal stability, with only 2 of 11 MEAs showing long-term stability. Several other studies have also reported the occurrence of MEA signal loss or recording failure over time [55]. There are multiple culprits for why MEAs experience recording failure over time, including the brain FBR or reasons not attributed to the FBR, such as leakiness of the BBB and astrogliosis [42]. The MEA failure could also be attributed to factors such as infection [56], connector failure [55b], or MEA degradation [57]. However, the exact mechanisms of MEA recording failure are not entirely clear [42].

4. Microelectrode Array Modifications for Improving the Neural Interface and Reducing the Foreign Body Response

Clinical application of NISs is limited due to the tendency of MEAs to elicit a prolonged immune response and to the fact that they experience loss in performance over time. Therefore, in order to apply NIS technology on a large scale, the FBR following MEA implantation must be substantially reduced to allow successful neural interfacing and maintaining MEA functionality. Several strategies have been applied in the past to promote integration of MEAs into the brain, including altering their surface topography, geometry, and stiffness, along with application of biomimetic coatings and drug/gene delivery [58]. The following sections discuss several approaches for modifying MEAs in reducing the FBR and maintaining a stable neural interface. The strategies for improving microelectrode arrays have also been summarized in Table 1.

4.1. Surface Modification

Upon MEA insertion, the first thing brain tissues and cells will come into contact with is the surface of the MEA. Thus, characteristics of the MEA surface will have significant impact on the progression of the resulting FBR. Notable surface modifications to MEAs include alterations of both surface chemistry and topography, which influence the ability of neuronal cells and proteins to adhere (cells) or adsorb (proteins) to the MEA surface, along with the ability of neuronal cells to proliferate and repair the site of injury. The degree of glial interaction with the MEA surface can also be influenced considerably through MEA surface chemistry and topography alterations.

4.1.1. Surface Chemistry Modification—In the context of this paper, MEA surface chemistry refers to chemical substances used to augment biocompatibility or stability of the MEA surface. Depending on chemical compositions, they can affect the types of intermolecular forces interacting with neural cells and proteins, such as hydrophobic/hydrophilic interactions (proteins preferentially adhere to hydrophobic surfaces) [39, 59], or how glial cells interact with the MEA during an FBR. A common approach for modifying surface chemistry of MEAs is through application of various neurointegrative coatings, which may include extracellular matrix (ECM) components, as well as synthetic chemicals and polymers intended for improving neural cell adhesion to the MEA surface, reducing gliosis and subsequent glial scaring, or increasing MEA longevity (Figure 3A). Hydrogels have also been applied to MEAs in attempt to improve their biocompatibility.

The ECM is of paramount importance for proper functioning of both cells and tissues, given it serves as a structural element and possesses various components, such as proteins, that allow for cells to facilitate focal adhesions with their surrounding environment [39]. ECM based coatings can serve as a biomimetic substitute for native ECM in the brain, allowing for facilitation of stronger cellular adhesion to the surface of the MEA. Additionally, it has been shown that the ECM exhibits both hemostatic and immunomodulatory properties [60]. In one study [61], the effectiveness of clinically approved neurosurgical hemostatic coating (Avitene™-MCH) was compared with an ECM coating obtained from astrocytes in rat brains on suppressing resulting FBR following the implantation of MEAs. It was discovered

that both coatings possessed accelerative effects on the coagulation cascade, but the coating obtained from rat astrocytes also possessed microglial suppressive properties. Moreover, the astrocyte-based coating reduced severity of astrogliosis 8 weeks following MEA implantation (Figure 3, B1–B4). In another study, Ceyssens *et al.* [62] assessed the effectiveness of a temporary coating of ECM proteins, which were obtained from thin slices of porcine gut tissue, on interfacing MEAs with brain tissue. Compared to an uncoated control MEA, the MEA with the ECM protein coating showed no significant damage to surrounding brain tissue 3 months following implantation. Coatings of ECM derived poly-D-lysine (PDL) and neuroadhesive L1 have also been shown to impact biocompatibility of MEAs in a significant way. Ghane-Motlagh *et al.* [63] tested the effectiveness of PDL coatings on increasing neural cell adhesion and proliferation on the surface of silicon MEAs coated with polyethylene glycol (PEG) and Perylene-C. It was discovered that neuroblast cells cultured on the MEA surface preferred to grow on the tips coated with PDL compared to uncoated MEAs. In a study by Eles *et al.* [64], the effectiveness of neuroadhesive L1 coatings on attenuating the attachment of microglia to MEAs was tested. Results indicated that in comparison to uncoated MEAs, MEAs coated with neuroadhesive L1 showed statistically significant 83% reduction in the number of microglia attached to the MEA surface. Several other studies have also indicated success in using neuroadhesive L1 to enhance MEA biocompatibility [65].

Although natural ECM shows great beneficial effects when applied on the MEA surfaces, there have been past instances where naturally derived ECM polymers exhibited immunogenicity because of the high temperature caused molecular changes during the implant fabrication process. Additionally, molecular structure variability is to be expected when deriving ECM coating materials from other species, such as animals, which may further cause issues including pathogen transfer [9d]. To develop more biocompatible, longer lasting MEAs, it may be necessary to use coatings other than those derived naturally as a result of said variability, such as synthetic polymers or naturally occurring polymers derived through synthetic means. This would allow each polymer to be tailored to the patient's natural brain environment, possibly resulting in a significant increase in MEA biocompatibility. Alternatively, cell-derived ECM could be applied to MEAs to improve biocompatibility, as ECM secreted from cells more closely resembles native ECM. This reduces the likelihood of a negative immunological response such as that seen when using animal tissue-derived ECM, which is structurally different both physically and chemically from native human ECM.

MEA biocompatibility can also be improved through synthetic means, such as using polymer or chemical MEA coatings to facilitate cellular adhesion or attenuation of glial responses and improving MEA longevity. Capeletti *et al.* [66] tested the effectiveness of silica sol-gel coatings on supporting neural cell growth and reducing gliosis. Results indicated that the silica sol-gel coating was capable of preventing astrocyte growth, while simultaneously promoting adhesion and growth of neurons, which was an outcome resulting from the inclusion of aminopropyl groups within the gel. Polyionic nanocoatings, such as poly(3,4-ethylenedioxythiophene) (PEDOT) films, especially those with mixed ionic charges, show promise in both improving biocompatibility and signal maintenance of MEAs [67]. It should also be noted that nanomaterial and nanostructure modifications to the MEA surface have a

significant impact on their electrical conductivity when electroconductive materials are used. In a study by Kojabad *et al.* [68], MEAs were enhanced with nanostructural modifications by coating them with polypyrrol nanotubes augmented with gold nanoparticles, which led to a tenfold decrease in the electrochemical impedance compared to the uncoated control. Burblies *et al.* [69] coated platinum cochlear neural electrodes with carbon nanotubules (CNTs). The CNT coatings both reduced electrical impedance and increased MEA capacitance, while also allowing for stable cell growth. Additionally, biomimetic superoxide dismutase (SOD) coatings have been shown to successfully in improve MEA longevity. Potter-Baker *et al.* [70] observed the effects of reactive oxygen species on a hybrid Mn(iii)tetrakis(4-benzoic acid)porphyrin (MnTBAP)-antioxidant composite coating. It was shown that the hybrid surface coating provided several days of shielding against reactive oxygen species, while also simultaneously reducing microglial production of both intracellular and extracellular reactive oxygen species. Yet as with naturally derived polymers, such as those composing the ECM, care must be taken when using synthetic polymers or chemicals, as they can possibly become immunogenic or toxic.

Hydrogels are also an important form of above-mentioned MEA surface coatings in attempt to improve their biocompatibility through different mechanisms. In a study by Skousen *et al.* [71], sodium alginate hydrogels, intended for acting as diffusion sinks were attached to the MEAs in varying degrees of thickness. It was discovered that by increasing hydrogel coating thickness up to 400 μm, overall FBR can be significantly reduced. While the aforementioned study indicates that hydrogel coatings can be used to increase biocompatibility, concerns remain in the degradation of hydrogels over time. As said study was conducted only over the course of 16 weeks, the long-term efficacy of a hydrogel coating needs to be evaluated. Additionally, the thickness of a hydrogel coating can be optimized to minimize the insertion damage as well as severe FBR.

4.1.2. Topography Modification—Another component of the MEA surface that has an impact on biocompatibility of MEAs is topography, which influences the surface area available for protein adsorption (Figure 3C). The greater the exposed surface area, the more proteins will adsorb to the MEA surface [39], which can significantly improve cell adhesion to the MEA surface. The stability of cell adhesion will ultimately influence their proliferation [72]. Good cell adhesion and proliferation is key for the brain to be able to heal following MEA implantation and to prevent micromotion induced strain around the MEA. In one study by Liu *et al.* [59a], the effects of both MEA topography on protein adsorption, specifically the adsorption of albumin, fibrinogen, and platelets, were tested. The applied microscale pillar structure influenced both platelet adhesion and activation, with topographic structures (interspacing of 6-8 μm) more similar to platelet size (2-3 μm) [73] successfully inhibiting these processes. Additionally, studies have also shown that nanoporous MEAs, such as those fabricated through the inclusion of nanoporous gold [74], can successfully reduce astrocytic coverage of the MEA surface (Figure 3, D1–D4), reduce scar tissue formation, and improve neuronal coverage. It was specified that the topography, not the surface chemistry of the MEAs, facilitated these improvements. This may be explained by the unique interactions of different cell types to different nanofeature size ranges through focal adhesions [75].

However, in some cases, topographic alterations do not have significant impact on enhancing biocompatibility. Bérces *et al.* [76] demonstrated that neural cells preferred binding to each other rather than the nanopatterned silicon and platinum MEA surfaces. Also, a study performed by Ereifej *et al.* [77] tested the effects of nanopatterned parallel grooves (200nm wide and 200nm deep with 300nm spacing between) on MEA biocompatibility, specifically through determination of the overall inflammatory response. Results indicated that in comparison to the control, non-patterned, MEA surfaces, the nanopatterned grooves did not significantly reduce neuroinflammation. Topographical dimensions on an MEA surface may also determine how well neural cells will be able to bind to the MEA. One study [78] demonstrated that MEA surfaces covered with 580-800 nm long nanopillars with 150-200 nm diameter exhibited less severe gliosis and more stable neuronal density in comparison to other examined surface topographies: (1) 2 μm surface patterns on unpolished silicon wafers, (2) polycrystalline silicon (grain size of 100-200 nm) possessing 1.04 surface roughness factor, and (3) fluorocarbon polymer coated 1-2 μm ridges. Nevertheless, topographic alterations alone may not have a pronounced effect on improving MEA biocompatibility, unless combined with additional factors. Combining nanoscale pores and microscale grooves with a PEDOT coating has been shown to not only reduce interfacial impedance, but also provide a favorable, non-toxic environment for neuronal growth [79]. It is also possible that the material from which the MEA is fabricated could compromise the biocompatibility and performance of the MEA even after its topographical alterations. Materials utilized to fabricated MEAs in most of the aforementioned studies [59a, 74, 76–77, 79] were primarily very stiff materials, such as platinum, silicon, glass, and stainless metals. Given neuronal cells have considerable difficulty in attaching to stiff surfaces, it comes to no surprise that success is not always guaranteed when applying surface topography enhancements to stiff substrates. To further enhance the efficacy of applying topographic alterations to MEA surfaces, it would be highly beneficial to use substrates with significantly lower stiffness ratings to apply and test the effectiveness of different topographies in improving MEA biocompatibility and longevity.

4.2. Surface Geometry Modification

Manipulating various geometrical factors of the MEA can result in difference in the FBR across cellular and tissue scales. These can also be the result of desires to use novel manufacturing methods to add features or manufacturing ease. Factors including the length, aspect ratio, and shape of the shank could all have an impact on the injury due to insertion, mechanical behavior, and long-term injury response. The shapes vary from the inclusion of pillars, or rods to create flat, round, or square pointed shanks (Figure 3E) [80]. Previously, there have been studies examining and comparing a variety of existing array configurations, however a comprehensive systematic evaluation of the geometric features has not been performed on currently relevant devices. Some of the most studied array geometries include the Utah array (Figure 2B) and the Michigan array (Figure 2C) [80–81], as they offer advantages over more traditional microwire electrode designs, such as noise reduction, increased ease of recording site definition, and reduction in the number of microdrives required to implant the electrode into the brain [82]. Utah arrays are characterized by grids of silicon microelectrodes, each of which are approximately 1 mm in length, with intermediate spacings of 0.4 mm and a surface area of about 12.96 mm^2 [83]. Additionally, Parylene-C is

used to coat the surface of Utah electrodes, which acts to insulate the electrode. Also, iridium is deposited on the tips of each microelectrode to facilitate signal transduction [84]. Michigan electrodes are characterized by the presence of 16 recording sites arranged in a quad shank configuration fabricated from a silicon substrate. Each shank is approximately 3 mm long, coated with a silicon dioxide/nitride insulating layer. The entire Michigan electrode possesses a surface area of approximately 1.25 mm^2 [80]. One major difference between these two is their production method resulting in either a 2D or 3D geometry. The 2D geometry of the Michigan electrode implies that it has less effective sensing area, reducing its sensitivity. However, the Michigan electrode offers several benefits, such as the ability to use silicon wafer manufacturing techniques to create channels or internal geometries/features within each electrode [85]. Additionally, the shanks can be manufactured to nearly any length, offering opportunities to obtain deeper signals.

Utah arrays are often shorter, as they are machined from the depth of a single sheet of silicon or metal. This limits their depth to a few millimeters, but also reduces their overall profile, often making them more practical for being placed in close proximity to the skull by reducing the proclivity for micromotions caused by exceeding the 1-2.5 mm subarachnoid space and coming in contact with bone [86]. Precision machining can also result in a dense array, resulting in higher resolution than is typically achieved using 2D methods. In a brief examination of these primary categories, Karumbaiah *et al.* [87] used histology, cytokines, and electrophysiology to demonstrate some of the differences between these geometries. They found that small electrodes (15μm Michigan electrodes and microwire electrodes) reduces glial scarring markers, while cylindrically shaped wire shanks help to mitigate long term FBR by limiting BBB breach. Another study [88] demonstrated that cylindrically shaped neural probes are feasible for maintaining single unit and multiunit activity long-term and were also shown to elicit a less severe FBR compared to other MEA geometries (Figure 3, F1–F3), such as those utilized in focal epilepsy treatment. Floating, untethered MEAs (Figure 2A) have also shown promise in reducing FBR severity (Figure 3, F4 & F5) [89]. Other applications of geometric manipulation have been utilized to increase biocompatibility, such as creating synapse like structures (i.e. “nanoedges” mimicking the post synaptic cleft), and precise curvatures to increase electrical activity, though these are generally limited to surface features on planar electrodes [90], including topography and surface chemistry.

Furthermore, initial research has begun in using more advanced manufacturing techniques, such as 3D printing, to overcome the limitations of existing methods and combine some of the benefits of both Utah and Michigan arrays. Because additive manufacturing is being used, the length of the shank could be specified, limited only by the mechanical properties of the material. The shape and density of the shanks could be similarly controlled, depending on the resolution of the printing system used. As demonstrated by Roberts *et al.* [91], current technology allows for printing with resolutions of 5um vertical and 30 um lateral which has allowed them to mimic current array geometries for a 10×10 MEA consisting of 1.5 mm tapered electrodes. Further development of this technique could allow for the creation of 3D shanks of almost any geometry and length. An added benefit of this could be that it would remove the dependence on the stock materials currently used for longer electrodes (i.e. silicon), which are characterized by vastly different mechanical properties to that of brain

tissue, and instead allow for the development of polymer and metal shanks with improved biocompatibility.

4.3. Stiffness Modification

One of the most important aspects regarding MEAs that determines their biocompatibility is mechanical properties, especially stiffness. As aforementioned, cells and tissues of the brain are characterized by a Young's modulus of approximately 3 kPa, whereas MEAs are characterized by Young's moduli ≥60 GPa, depending on the material used to fabricate them [5–8]. Because of this large stiffness difference, cells are unable to pull on and stretch MEAs like they would normal brain substrate, preventing them from forming as many focal adhesions and increasing instability [50], ultimately resulting in a more severe FBR. However, by matching mechanical properties of MEAs with brain tissue, the FBR can be substantially reduced.

When designing flexible, soft MEAs, multiple factors must be considered regarding the material. Because neural MEAs are intended for a low stress, highly compliant environment, factors such as overall MEA yield strength, tensile strength, ductility, and toughness are arguably less important than MEA resilience and elasticity (i.e. neural cells need to be able to pull on and easily deform the MEA, but not permanently). Thereby, to increase MEA mechanical compliance, polymers are frequently used, as they can achieve a significantly lower Young's modulus in comparison to metals, and elasticity can be introduced into the material. Sohal *et al.* [92] compared the severity of the FBR elicited when implanting two different types of MEAs into the brains of white rabbits: a stiff, nonflexible microwire MEA and a flexible, Parylene-C sinusoidal MEA. Both microglial and astrocytic responses were significantly lowered for the flexible sinusoidal MEA compared to the nonflexible microwire MEA surrounding the site of implantation. In another study, Luan *et al.* [93] observed the performance of ultraflexible nanoelectric thread (UNET) electrodes in reducing overall FBR. It was discovered that UNET electrodes achieved highly successful neural integration, with minimal glial scaring and full recovery of the BBB integrity. Several other studies have also reported significant reduction in FBR severity through alterations of MEA flexibility [94]. In a few cases, MEAs have been developed with stiffness moduli in the range of kPa (more closely resembling the brain tissue Young's modulus range), which is significantly smaller than that seen in the more common silicon MEAs. Du *et al.* [95] developed ultrasoft MEAs with Young's moduli less than 1 MPa and implanted them into rat brains to test their effectiveness in mitigating the FBR compared to a stiffer MEA with similar geometry and surface properties. The ultrasoft MEAs were far more superior to that of the stiff MEAs regarding FBR severity and tissue integration. In another study [96], extremely soft and compliant polypyrrol MEAs with low Young's moduli (450 kPa), along with good stretchability, conductive properties, and substrate adhesion, were successfully developed. Ischiadic nerve stimulation in rats was also achieved using the polypyrrol MEAs. Given the large amount of data supporting the efficacy of using soft, flexible materials in the manufacture of MEAs, it would be highly beneficial to select materials that more closely resemble the brain tissue Young's modulus for MEA manufacturing.

With softer, more flexible MEAs, however, comes additional difficulty in inserting them into the brain. Nevertheless, it is possible to alter mechanical properties of MEAs, so they are stiffer upon implantation to aid penetration, but become flexible following implantation (Figure 3G). Kil *et al.* [97] used a dextran coating with a thickness of 37 μm and bending stiffness of 10.5 ± 5.5 $N \cdot m^{-1}$ (Young's modulus of 0.6 ± 0.1 GPa) to temporarily stiffen flexible MEAs before insertion. The resulting FBR and glial scar formation following implantation of the dextran coated MEAs was shown to be very minimal, with neurons infiltrating the dextran coating site following dissolution (Figure 3, H1 & H2). In a study by Agorelius *et al.* [98], flexible MEAs were encased in a hard gelatin coating to aid in penetration, which would dissolve following MEA implantation. It was found that after several weeks following implantation, signals obtained from each MEA remained relatively stable, indicating that the gelatin coating prevented the MEA from becoming damaged during implantation. Khilwani *et al.* [94a] developed stiff dissolvable needles for small, compliant MEAs, which allowed insertion without mechanical failure and successful dissolution of the needle following implantation. Another study [99] tested the feasibility of using an ultrafast biodegrading polycarbonate (E5005(2K)) polymer coating (Young's modulus = 1.6 GPa) for aiding in flexible Parylene MEA insertion. MEA probes of varying size and polymer coat thickness were implanted into rat brains, and an assessment of subsequent FBR and neural cell loss was performed. It was shown that small MEAs with appropriate coat thickness were characterized by less damage and a less severe FBR. Ultimately, the less damage caused upon insertion, the less severe the FBR will become.

Nguyen *et al.* [94b] tested the effectiveness of an MEA designed to be rigid initially, but becoming compliant following insertion, on reducing FBR severity. It was shown that the acute FBR characteristic of the mechanically adaptive MEA was similar to that seen from a permanently stiff MEA, but over time, the mechanically adaptive MEA resulted in a less severe FBR compared to stiff MEAs. In a study performed by Hess-Dunning *et al.* [100], MEAs composed of biomimetic mechanically-softening polymer nanocomposite were monitored for device and recording failure over the course of several weeks. MEA recording signals remained stable throughout the entire study. Another study by Potter *et al.* [101] tested the feasibility of not only applying mechanically adaptive polymers in MEA design, but upon softening of the MEA, being able to deliver local administrations of antioxidants, such as curcumin. The multiprong MEA design of mechanical softening and curcumin release resulted in higher neuronal survival and increased BBB stability. Taken together, reducing MEA stiffness, increasing MEA flexibility, and increasing ease of MEA insertion all have significant impact on MEA biocompatibility and recording performance.

Additionally, it may also be possible to modify mechanical properties of MEAs through the application of soft, compliant hydrogel surface coatings, rather than changing mechanical properties of the entire MEA (Figure 3G). Spencer *et al.* [102] developed polyethylene glycol dimethacrylate (PEG-DMA) hydrogel coatings for MEAs with thicknesses ranging from 25-100 μm and mechanical properties (Young's modulus of 11.6 kPa) similar to that of the brain tissue. *In vivo* testing of the PEG-DMA hydrogels showed that MEAs coated with hydrogels experienced significantly reduced strain caused by micromotion and glial scaring compared to hard, uncoated MEAs (Figure 3, H3–H5). Therefore, hydrogel coatings may be viable options for improving performance and biocompatibility of MEAs. However, as

aforementioned, hydrogels tend to degrade over time, so the long-term efficacy of using such a mechanically matched hydrogel in MEA design needs to be further assessed.

5. Future Outlook

Presently, most MEAs used in clinical applications are fabricated primarily using metallic substances such as silicon, tungsten, and glass [4]. A major issue with these materials is substantial differences in Young's moduli between themselves and the brain tissue [5–8]. Also, differences in chemical properties cause additional problems with MEA biocompatibility, such as reduced cell adhesion and proliferation. As a result, without good cell adhesion, MEAs are free to move around in the brain, causing additional strain on the surrounding tissue [41b]. Not only does this cause damage to the brain, but it also compromises MEA function over time [42, 54]. Adding to this problem is the ensuing FBR following MEA insertion. Both prolonged microglial activation and formation of a glial scar cause issues for brain tissue and the MEA itself [42, 48]. Nevertheless, various modifications to MEAs have been shown to be highly successful in reducing the resulting FBR following MEA insertion and improving their performance. Applying modifications to surface chemistry, topography [59a, 61, 67b], stiffness [92, 96, 100], and geometry [81, 86, 90a] of MEAs have all been shown to be highly promising for improving MEA biocompatibility.

Although each of these modifications can mitigate the resultant FBR to some extent, the FBR still lasts, which will cause issues with the MEA. In order to substantially reduce severity of the FBR and maintain the signal transduction from an MEA, multiple different factors must be considered. The most logical approach would be to implement a multiprong MEA design by combining the modifications to surface properties, mechanical properties, and geometry. Also, to further improve MEA integration, it may be possible to implement additional factors beyond that of MEA design, such as therapeutic drugs. One example is the intravenous injection of the trefoil factor 3 (TFF3) protein (a protein upregulated in the liver in response to neural injury), which has been shown to possess neuroprotective properties, and is capable of diffusing through the BBB [103]. Another strategy is to implement stem cell therapies following MEA insertion. One example is mesenchymal stem cells (MSCs), which possess both immunomodulatory (cytokine induced nitric oxide production) [104] and tropic activity (inhibition of apoptosis and fibrosis/scaring, angiogenesis stimulation, anti-inflammatory) [105], and could increase the speed of healing and reduce FBR severity. The fact that stem cells, such as human adipose-derived stem cells (hASCs) [106], are fully capable of passing through the BBB makes this an even more viable option. However, therapies involving stem cells are still in the developmental phase, and there is a considerable resistance to implementing them on a large scale. Nevertheless, further development of MEAs and NISs will likely yield considerable rewards and improve the lives of innumerable individuals.

6. Summary

There is considerable interest in applications of NISs, given they have the potential to improve lives of individuals possessing severe neurological complications. However, the inherent mechanical and chemical mismatch between brain tissue and MEAs results in

several undesirable effects, such as MEA micromotion and FBR. This not only causes damage and alterations to the brain, but also compromises MEA functionality, which ultimately leads to NIS malfunction over time. Therefore, various properties of implanted MEAs must be modified in order to meet the needs for large-scale clinical applications. Application of surface coatings (natural/synthetic) and topographical modifications to MEA design have been highly successful in reducing FBR severity, increasing neuronal survival, and boosting both MEA signal maintenance and longevity. Modifications to both MEA geometry and mechanical properties have also shown significant success in FBR reduction, increasing MEA service life, etc. However, these modifications do not always have a pronounced effect on MEA biocompatibility or overall performance. Because some approaches to MEA modification (i.e. nanopatterned grooves and Avitene™-MCH) are limited in their ability to improve neurological integration and host tolerance individually, this must be considered when designing newer generations of MEAs. Future MEA designs should incorporate all three aforementioned property modifications as well as the inclusion of external factors, such as drug delivery and stem cell therapies, to ensure maximum biocompatibility and overall performance.

Acknowledgements

This study was supported by the National Institutes of Health (1R15CA202656 and 1R15HL145654) and the National Science Foundation (1703570) to FZ. It was also supported by the Portage Health Foundation to both FZ and DS.

References

[1]. National Spinal Cord Injury Statistical Center (NSCISC), Spinal Cord Injury (SCI) Facts and Figures at a Glance, https://www.nscisc.uab.edu/Public/Facts%202016.pdf, accessed: April 21, 2019.

[2]. Hatsopoulos NG, Donoghue JP, Annual Review of Neuroscience 2009, 32, 249.

[3]. Ziegler-Graham K, MacKenzie EJ, Ephraim PL, Travison TG, Brookmeyer R, Archives of Physical Medicine and Rehabilitation 2008, 89, 422. [PubMed: 18295618]

[4]. a)Zhang S, Y. Song, Wang M, Zhang Z, Fan X, Song X, Zhuang P, Yue F, Chan P, Cai X, Biosensors and Bioelectronics 2016, 85, 53; [PubMed: 27155116] b)Musallam S, Bak MJ, Troyk PR, Andersen RA, Journal of Neuroscience Methods 2007, 160, 122; [PubMed: 17067683] c)Kipke DR, Vetter RJ, Williams JC, Hetke JF, IEEE Transactions on Neural Systems and Rehabilitation Engineering 2003, 11, 151; [PubMed: 12899260] d)Gagne S, Plamondon R, IEEE Transactions on Biomedical Engineering 1987, BME-34, 56.

[5]. Hopcroft MA, Nix WD, Kenny TW, Journal of Microelectromechanical Systems 2010, 19, 229.

[6]. Hand RJ, Tadjiev DR, Journal of Non-Crystalline Solids 2010, 356, 2417.

[7]. Qiu KQ, Wang AM, Zhang HF, Ding BZ, Hu ZQ, Intermetallics 2002, 10, 1283.

[8]. a)Elkin BS, Azeloglu EU, Costa KD, B. M III, Journal of Neurotrauma 2007, 24, 812; [PubMed: 17518536] b)Saxena T, Gilbert JL, M. J Hasenwinkel, 2009, 90A, 1206.

[9]. a)Anderson JM, Annual Review of Materials Research 2001, 31, 81;b)Anderson JM, Rodriguez A, Chang DT, Seminars in Immunology 2008, 20, 86; [PubMed: 18162407] c)Luttikhuizen DT, Harmsen MC, Luyn MJAV, Tissue Engineering 2006, 12, 1955; [PubMed: 16889525] d)Morais JM, Papadimitrakopoulos F, Burgess DJ, The AAPS Journal 2010, 12, 188. [PubMed: 20143194]

[10]. Allen NJ, Barres BA, Nature 2009, 457, 675. [PubMed: 19194443]

[11]. Leboffe MJ, A Photographic Atlas of Histology, Morton Publishing Company, Englewood, CO 2013.

[12]. Hilgetag CC, Barbas H, Brain Structure and Function 2009, 213, 365. [PubMed: 19198876]

[13]. Azevedo FAC, Carvalho LRB, Grinberg LT, Farfel JM, Ferretti REL, Leite REP, Filho WJ, Lent R, Herculano-Houzel S, Journal of Comparative Neurology 2009, 513, 532. [PubMed: 19226510]

[14]. Purves D, Augustine G, Fitzpatrick D, Hall W, LaMantia A, McNamara J and Williams S, Neuroscience, Sinauer Associates, Inc, Sunderland, MA 2004.

[15]. Nicholls JG, Martin A, Wallace B and Fuchs P, From Neuron to Brain Sinauer Associates, Inc., Sunderland, MA 2001.

[16]. Block ML, Zecca L, Hong J-S, Nature Reviews Neuroscience 2007, 8, 57. [PubMed: 17180163]

[17]. Kim SU, de Vellis J, Journal of Neuroscience Research 2005, 81, 302. [PubMed: 15954124]

[18]. Hanisch U-K, Kettenmann H, Nature Neuroscience 2007, 10, 1387. [PubMed: 17965659]

[19]. Mittelbronn M, Dietz K, Schluesener HJ, Meyermann R, Acta Neuropathologica 2001, 101, 249. [PubMed: 11307625]

[20]. Lawson LJ, Perry VH, Dri P, Gordon S, Neuroscience 1990, 39, 151. [PubMed: 2089275]

[21]. Verkhratsky A, Butt A, Glial Physiology and Pathophysiology, Wiley, 2013.

[22]. Dong Y, Benveniste EN, Glia 2001, 36, 180. [PubMed: 11596126]

[23]. Chen Y, Swanson RA, Journal of Cerebral Blood Flow & Metabolism 2003, 23, 137. [PubMed: 12571445]

[24]. a)C. Farina, F. Aloisi, E. Meinl, Trends in Immunology 2007, 28, 138; [PubMed: 17276138] b)Ridet JL, Privat A, Malhotra SK, Gage FH, Trends in Neurosciences 1997, 20, 570. [PubMed: 9416670]

[25]. Baumann N, Pham-Dinh D, Physiological Reviews 2001, 81, 871. [PubMed: 11274346]

[26]. Del Bigio MR, Acta Neuropathologica 2010, 119, 55. [PubMed: 20024659]

[27]. Polikov VS, Tresco PA, Reichert WM, Journal of Neuroscience Methods 2005, 148, 1. [PubMed: 16198003]

[28]. Joshua E. Burda, Michael V. Sofroniew, Neuron 2014, 81, 229. [PubMed: 24462092]

[29]. Färber K, Kettenmann H, Brain Research Reviews 2005, 48, 133. [PubMed: 15850652]

[30]. a)Babcock AA, Kuziel WA, Rivest S, Owens T, The Journal of Neuroscience 2003, 23, 7922; [PubMed: 12944523] b)Chabot S, Williams G, Yong VW, The Journal of Clinical Investigation 1997, 100, 604; [PubMed: 9239408] c)Nakajima K, Honda S, Tohyama Y, Imai Y, Kohsaka S, Kurihara T, Journal of Neuroscience Research 2001, 65, 322. [PubMed: 11494368]

[31]. Kozai TDY, Vazquez AL, Weaver CL, Kim S-G, Cui XT, Journal of neural engineering 2012, 9, 066001. [PubMed: 23075490]

[32]. Stence N, Waite M, Dailey ME, Glia 2001, 33, 256. [PubMed: 11241743]

[33]. Kozai TDY, Gugel Z, Li X, Gilgunn PJ, Khilwani R, Ozdoganlar OB, Fedder GK, Weber DJ, Cui XT, Biomaterials 2014, 35, 9255. [PubMed: 25128375]

[34]. a)Landis DMD, Annual Review of Neuroscience 1994, 17, 133;b)Sofroniew MV, Trends in Neurosciences 2009, 32, 638. [PubMed: 19782411]

[35]. Sofroniew MV, Vinters HV, Acta Neuropathologica 2010, 119, 7. [PubMed: 20012068]

[36]. Szarowski DH, Andersen MD, Retterer S, Spence AJ, Isaacson M, Craighead HG, Turner JN, Shain W, Brain Research 2003, 983, 23. [PubMed: 12914963]

[37]. Kozai TDY, Langhals NB, Patel PR, Deng X, Zhang H, Smith KL, Lahann J, Kotov NA, Kipke DR, Nature materials 2012, 11, 1065. [PubMed: 23142839]

[38]. Stichel CC, Müller HW, Cell and Tissue Research 1998, 294, 1. [PubMed: 9724451]

[39]. Dee KC, Puleo DA, Bizios R, An Introduction to Tissue-Biomaterial Interactions John Wiley & Sons, Inc., Hoboken, New Jersey 2002.

[40]. Bennett C, Mohammed F, Álvarez-Ciara A, Nguyen MA, Dietrich WD, Rajguru SM, Streit WJ, Prasad A, Biomaterials 2019, 188, 144. [PubMed: 30343257]

[41]. a)Karumbaiah L, Norman SE, Rajan NB, Anand S, Saxena T, Betancur M, Patkar R, Bellamkonda RV, Biomaterials 2012, 33, 5983; [PubMed: 22681976] b)Lee H, Bellamkonda RV, Sun W, Levenston ME, Journal of Neural Engineering 2005, 2, 81. [PubMed: 16317231]

[42]. Nolta NF, Christensen MB, Crane PD, Skousen JL, Tresco PA, Biomaterials 2015, 53, 753. [PubMed: 25890770]

[43]. Obermeier B, Daneman R, Ransohoff RM, Nature medicine 2013, 19, 1584.

[44]. a)Hawkins BT, Davis TP, Pharmacological Reviews 2005, 57, 173; [PubMed: 15914466] b)Freeman LR, Keller JN, Biochimica et Biophysica Acta (BBA) - Molecular Basis of Disease 2012, 1822, 822; [PubMed: 22206999] c)Lifshitz J, Sullivan PG, Hovda DA, Wieloch T, McIntosh TK, Mitochondrion 2004, 4, 705. [PubMed: 16120426]

[45]. Bennett C, Samikkannu M, Mohammed F, Dietrich WD, Rajguru SM, Prasad A, Biomaterials 2018, 164, 1. [PubMed: 29477707]

[46]. Winterbourn CC, Toxicology Letters 1995, 82-83, 969. [PubMed: 8597169]

[47]. Graeber MB, Streit WJ, Acta Neuropathologica 2010, 119, 89. [PubMed: 20012873]

[48]. Biran R, Martin DC, Tresco PA, Experimental Neurology 2005, 195, 115. [PubMed: 16045910]

[49]. McKee CT, Last JA, Russell P, Murphy CJ, Tissue Engineering Part B: Reviews 2011, 17, 155. [PubMed: 21303220]

[50]. Discher DE, Janmey P, Y.-l. Wang, Science 2005, 310, 1139. [PubMed: 16293750]

[51]. Biran R, Martin DC, Tresco PA, Journal of Biomedical Materials Research 2007, 82A, 169.

[52]. Yin X, Zhang W, Yu Q, Shanghai Ligong Daxue Xuebao/Journal of University of Shanghai for Science and Technology 2018, 40, 539.

[53]. Ma YK, Zhang WG, Li ZW, Shanghai Jiaotong Daxue Xuebao/Journal of Shanghai Jiaotong University 2015, 49, 1882.

[54]. Debnath S, Prins NW, Pohlmeyer E, Mylavarapu R, Geng S, Sanchez JC, Prasad A, Biomedical Physics and Engineering Express 2018, 4.

[55]. a)Kozai TDY, Catt K, Li X, Gugel ZV, Olafsson VT, Vazquez AL, Cui XT, Biomaterials 2015, 37, 25; [PubMed: 25453935] b)Vetter RJ, Williams JC, Hetke JF, Nunamaker EA, Kipke DR, IEEE Transactions on Biomedical Engineering 2004, 51, 896; [PubMed: 15188856] c)Debnath S, Bauman MJ, Fisher LE, Weber DJ, Gaunt RA, Frontiers in Neurology 2014, 5, 1; [PubMed: 24454306] d)Saxena T, Karumbaiah L, Gaupp EA, Patkar R, Patil K, Betancur M, Stanley GB, Bellamkonda RV, Biomaterials 2013, 34, 4703. [PubMed: 23562053]

[56]. Barrese JC, Rao N, Paroo K, Triebwasser C, Vargas-Irwin C, Franquemont L, Donoghue JP, Journal of neural engineering 2013, 10, 066014. [PubMed: 24216311]

[57]. a)Prasad A, Xue Q-S, Sankar V, Nishida T, Shaw G, Streit WJ, Sanchez JC, Journal of Neural Engineering 2012, 9, 056015; [PubMed: 23010756] b)Schmitt G, Schultze JW, Faßbender F, Buß G, Lüth H, Schöning MJ, Electrochimica Acta 1999, 44, 3865.

[58]. Kozai TDY, Jaquins-Gerstl AS, Vazquez AL, Michael AC, Cui XT, ACS Chemical Neuroscience 2015, 6, 48. [PubMed: 25546652]

[59]. a)Liu Y, Zhang X, Hao P, Journal of Adhesion Science and Technology 2016, 30, 878;b)Yang Y, Cavin R, Ong JL, Journal of Biomedical Materials Research 2003, 67A, 344.

[60]. Lok J, Leung W, Murphy S, Butler W, Noviski N, Lo EH, in Acta Neurochirurgica, Supplementum, DOI: 10.1007/978-3-7091-0693-8_11, 2011, 63.

[61]. Oakes RS, Polei MD, Skousen JL, Tresco PA, Biomaterials 2018, 154, 1. [PubMed: 29117574]

[62]. Ceyssens F, Deprez M, Turner N, Kil D, Van Kuyck K, Welkenhuysen M, Nuttin B, Badylak S, Puers R, Journal of Neural Engineering 2017, 14.

[63]. Ghane-Motlagh B, Javanbakht T, Shoghi F, Wilkinson KJ, Martel R, Sawan M, Materials Science and Engineering: C 2016, 68, 642. [PubMed: 27524064]

[64]. Eles JR, Vazquez AL, Snyder NR, Lagenaur C, Murphy MC, Kozai TDY, Cui XT, Biomaterials 2017, 113, 279. [PubMed: 27837661]

[65]. a)Kolarcik CL, Bourbeau D, Azemi E, Rost E, Zhang L, Lagenaur CF, Weber DJ, Cui XT, Acta Biomaterialia 2012, 8, 3561; [PubMed: 22750248] b)Webb K, Budko E, Neuberger TJ, Chen S, Schachner M, Tresco PA, Biomaterials 2001, 22, 1017. [PubMed: 11352083]

[66]. Capeletti LB, Cardoso MB, Dos Santos JHZ, He W, ACS Applied Materials and Interfaces 2016, 8, 27553. [PubMed: 27715001]

[67]. a)Zhi B, Song Q, Mao Y, RSC Advances 2018, 8, 4779;b)Du ZJ, Luo X, Weaver CL, Cui XT, Journal of Materials Chemistry C 2015, 3, 6515; [PubMed: 26491540] c)Ludwig KA, Uram JD, Yang J, Martin DC, Kipke DR, Journal of Neural Engineering 2006, 3, 59. [PubMed: 16510943]

[68]. Kojabad ZD, Shojaosadati SA, Firoozabadi SM, Hamedi S, Journal of Solid State Electrochemistry 2019, 23, 1533.

[69]. Burblies N, Schulze J, Schwarz H-C, Kranz K, Motz D, Vogt C, Lenarz T, Warnecke A, Behrens P, PLOS ONE 2016, 11, e0158571. [PubMed: 27385031]

[70]. Potter-Baker KA, Nguyen JK, Kovach KM, Gitomer MM, Srail TW, Stewart WG, Skousen JL, Capadona JR, Journal of Materials Chemistry B 2014, 2, 2248. [PubMed: 25132966]

[71]. Skousen JL, Bridge MJ, Tresco PA, Biomaterials 2015, 36, 33. [PubMed: 25310936]

[72]. Lim JY, Hansen JC, Siedlecki CA, Runt J, Donahue HJ, Journal of The Royal Society Interface 2005, 2, 97.

[73]. Paulus JM, Blood 1975, 46, 321. [PubMed: 1097000]

[74]. Chapman CAR, Chen H, Stamou M, Biener J, Biener MM, Lein PJ, Seker E, ACS Applied Materials & Interfaces 2015, 7, 7093. [PubMed: 25706691]

[75]. Biggs MJ, Richards RG, Dalby MJ, Nanomedicine : nanotechnology, biology, and medicine 2010, 6, 619.

[76]. Bérces Z, Pomothy J, Horváth ÁC, Kohidi T, Benyei É, Fekete Z, Madarász E, Pongrácz A, Journal of Neural Engineering 2018, 15.

[77]. Ereifej ES, Smith CS, Meade SM, Chen K, Feng H, Capadona JR, Advanced Functional Materials 2018, 28, 1704420.

[78]. Bérces Z, Tóth K, Márton G, Pál I, Kováts-Megyesi B, Fekete Z, Ulbert I, Pongrácz A, Scientific Reports 2016, 6, 35944. [PubMed: 27775024]

[79]. Shi X, Xiao Y, Xiao H, Harris G, Wang T, Che J, Colloids and Surfaces B: Biointerfaces 2016, 145, 768. [PubMed: 27295493]

[80]. Ward MP, Rajdev P, Ellison C, Irazoqui PP, Brain Research 2009, 1282, 183. [PubMed: 19486899]

[81]. Szostak KM, Grand L, Constandinou TG, Frontiers in Neuroscience 2017, 11, 665. [PubMed: 29270103]

[82]. Cheung KC, Renaud P, Tanila H, Djupsund K, Biosensors and Bioelectronics 2007, 22, 1783. [PubMed: 17027251]

[83]. Kelly RC, Smith MA, Samonds JM, Kohn A, Bonds AB, Movshon JA, Lee TS, The Journal of neuroscience : the official journal of the Society for Neuroscience 2007, 27, 261. [PubMed: 17215384]

[84]. Kim S, Bhandari R, Klein M, Negi S, Rieth L, Tathireddy P, Toepper M, Oppermann H, Solzbacher F, Biomedical Microdevices 2009, 11, 453. [PubMed: 19067174]

[85]. Pei W, Chen H, DOI: 10.1007/978-981-10-5945-2_42 2018, p. 1437.

[86]. Cheng M-Y, Je M, Tan KL, Tan EL, Lim R, Yao L, Li P, Park W-T, Phua EJR, Gan CL, Yu A, Journal of Micromechanics and Microengineering 2013, 23, 095013.

[87]. Karumbaiah L, Saxena T, Carlson D, Patil K, Patkar R, Gaupp EA, Betancur M, Stanley GB, Carin L, Bellamkonda RV, Biomaterials 2013, 34, 8061. [PubMed: 23891081]

[88]. Fiáth R, Hofer KT, Csikós V, Horváth D, Nánási T, Tóth K, Pothof F, Böhler C, Asplund M, Ruther P, Ulbert I, Biomedizinische Technik 2018, 63, 301. [PubMed: 29478038]

[89]. Ersen A, Elkabes S, Freedman DS, Sahin M, Journal of Neural Engineering 2015, 12, 016019. [PubMed: 25605679]

[90]. a)Wijdenes P, Ali H, Armstrong R, Zaidi W, Dalton C, Syed NI, Scientific Reports 2016, 6, 34553; [PubMed: 27731326] b)Xie C, Lin Z, Hanson L, Cui Y, Cui B, Nature Nanotechnology 2012, 7, 185.

[91]. Roberts RC, Tien NC, presented at 2017 19th International Conference on Solid-State Sensors, Actuators and Microsystems (TRANSDUCERS), 18-22 June 2017, 2017.

[92]. Sohal HS, Clowry GJ, Jackson A, O'Neill A, Baker SN, PLOS ONE 2016, 11, e0165606. [PubMed: 27788240]

[93]. Luan L, Wei X, Zhao Z, Siegel JJ, Potnis O, Tuppen CA, Lin S, Kazmi S, Fowler RA, Holloway S, Dunn AK, Chitwood RA, Xie C, Science Advances 2017, 3.

[94]. a)Khilwani R, Gilgunn PJ, Kozai TDY, Ong XC, Korkmaz E, Gunalan PK, Cui XT, Fedder GK, Ozdoganlar OB, Biomedical Microdevices 2016, 18;b)Nguyen JK, Park DJ, Skousen JL, Hess-

Dunning AE, Tyler DJ, Rowan SJ, Weder C, Capadona JR, Journal of Neural Engineering 2014, 11;c)Lee HC, Ejserholm F, Gaire J, Currlin S, Schouenborg J, Wallman L, Bengtsson M, Park K, Otto KJ, Journal of Neural Engineering 2017, 14.

[95]. Du ZJ, Kolarcik CL, Kozai TDY, Luebben SD, Sapp SA, Zheng XS, Nabity JA, Cui XT, Acta Biomaterialia 2017, 53, 46. [PubMed: 28185910]

[96]. Qi D, Liu Z, Liu Y, Jiang Y, Leow WR, Pal M, Pan S, Yang H, Wang Y, Zhang X, Yu J, Li B, Yu Z, Wang W, Chen X, Advanced Materials 2017, 29, 1702800.

[97]. a)Kil D, Carmona MB, Ceyssens F, Deprez M, Brancato L, Nuttin B, Balschun D, Puers R, Micromachines 2019, 10;b)Kil D, Brancato L, Puers R, Journal of Physics: Conference Series 2017, 922, 012016.

[98]. Agorelius J, Tsanakalis F, Friberg A, Thorbergsson PT, Pettersson LME, Schouenborg J, Frontiers in Neuroscience 2015, 9.

[99]. Lo MC, Wang S, Singh S, Damodaran VB, Ahmed I, Coffey K, Barker D, Saste K, Kals K, Kaplan HM, Kohn J, Shreiber DI, Zahn JD, Journal of Neural Engineering 2018, 15.

[100]. Hess-Dunning A, Tyler DJ, Micromachines 2018, 9.

[101]. Potter KA, Jorfi M, Householder KT, Foster EJ, Weder C, Capadona JR, Acta Biomaterialia 2014, 10, 2209. [PubMed: 24468582]

[102]. Spencer KC, Sy JC, Ramadi KB, Graybiel AM, Langer R, Cima MJ, Scientific Reports 2017, 7.

[103]. Liu SQ, Roberts D, Zhang B, Ren Y, Zhang L-Q, Wu YH, PLOS ONE 2013, 8, e77732. [PubMed: 24204940]

[104]. Ren G, Zhang L, Zhao X, Xu G, Zhang Y, Roberts AI, Zhao RC, Shi Y, Cell Stem Cell 2008, 2, 141. [PubMed: 18371435]

[105]. Caplan AI, Dennis JE, Journal of Cellular Biochemistry 2006, 98, 1076. [PubMed: 16619257]

[106]. Kim S, Chang K-A, Kim J. a., Park H-G, Ra JC, Kim H-S, Suh Y-H, PLOS ONE 2012, 7, e45757. [PubMed: 23049854]

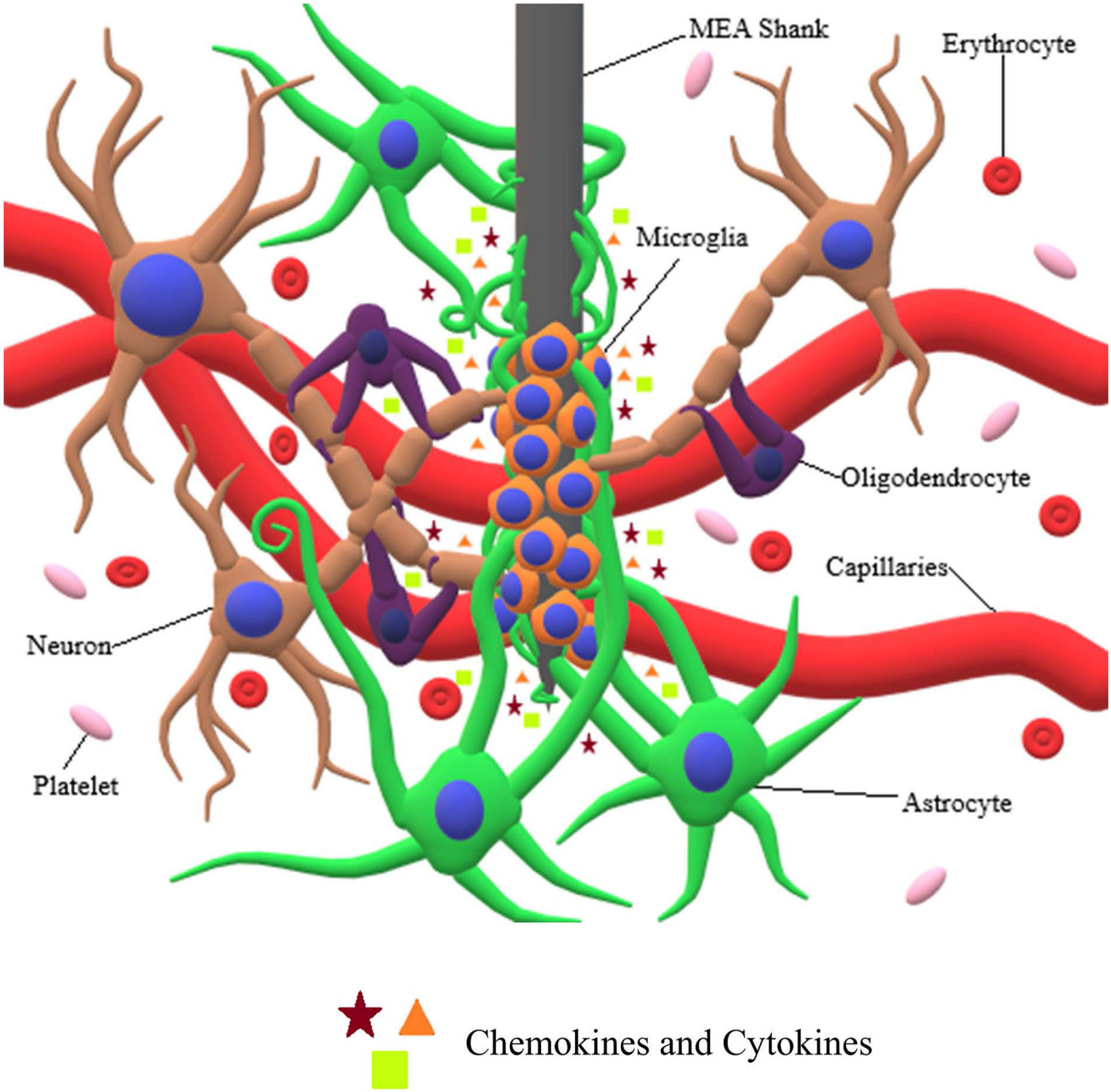

Figure 1:

Interaction of neuronal cells with MEA shank. MEA insertion causes severing of capillaries, cellular processes, and extracellular matrix, along with the release of erythrocytes and platelets. Additionally, the release of cytokines causes microglia and astrocytes to undergo morphological and behavioral changes. Microglia migrate towards the MEA shank and proceed to encapsulate it, while at the same time releasing proinflammatory cytokines and chemokine attractants. Following microglial encapsulation, astrocytes extend their processes towards the MEA shank, proceeding to encapsulate both the microglia and MEA shank.

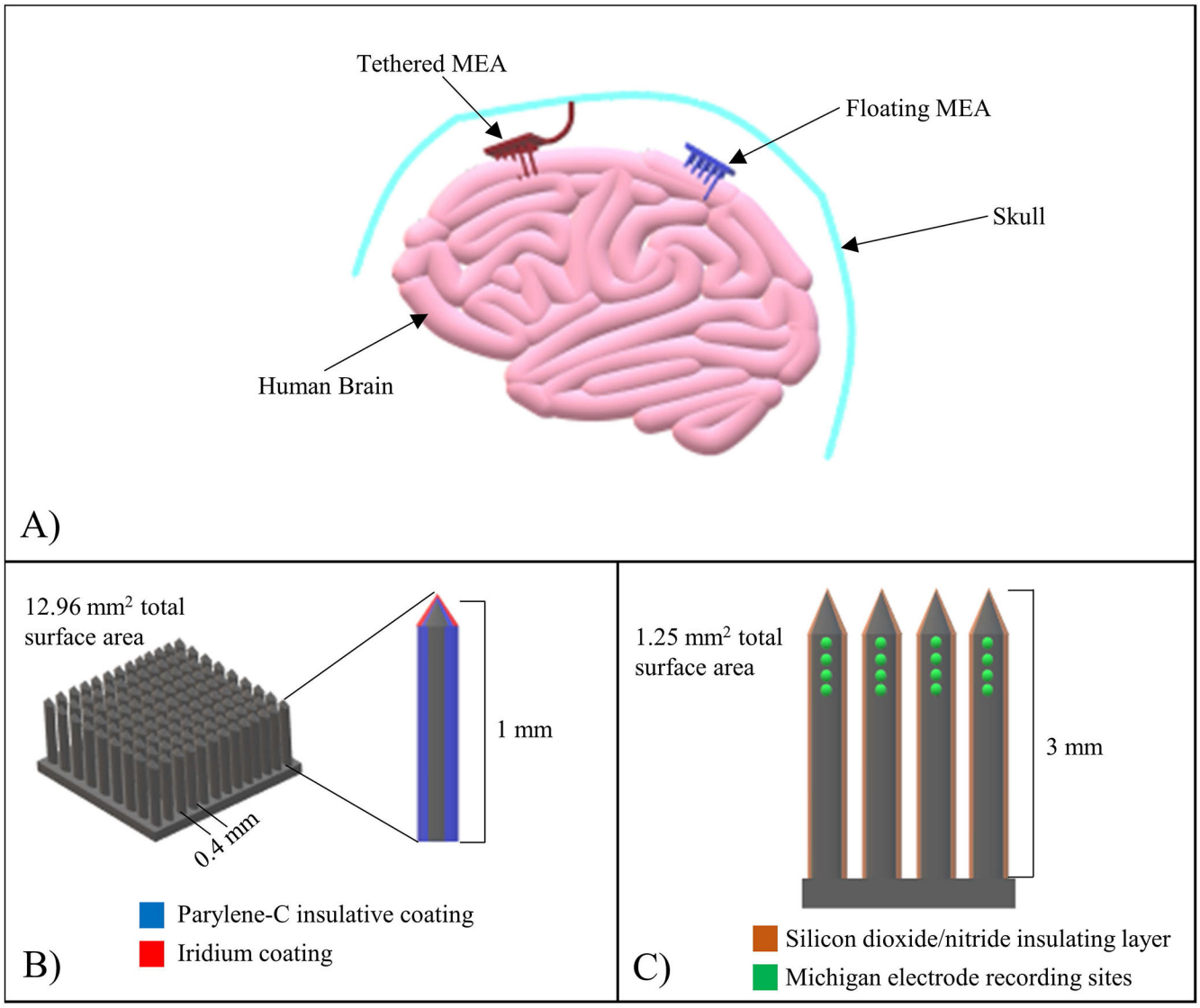

Figure 2:

MEA configuration examples. (A) Schematic demonstrating the difference between tethered and floating MEAs. Tethered MEAs, following implantation into the brain, are permanently attached to the skull to restrict movement, whereas floating MEAs are free to move around with the brain. (B) Schematic detailing the Utah MEA configuration. Grids of silicon electrodes 1 mm long, with 0.4 mm spacing and surface area of 12.96 mm^2, coated with Parylene-C and iridium. (C) Schematic detailing the Michigan MEA configuration. A quad shank arrangement with 16 recording sites, with each shank coated with silicon dioxide/nitride and measuring 3 mm in length (total surface area of 1.25 mm^2).

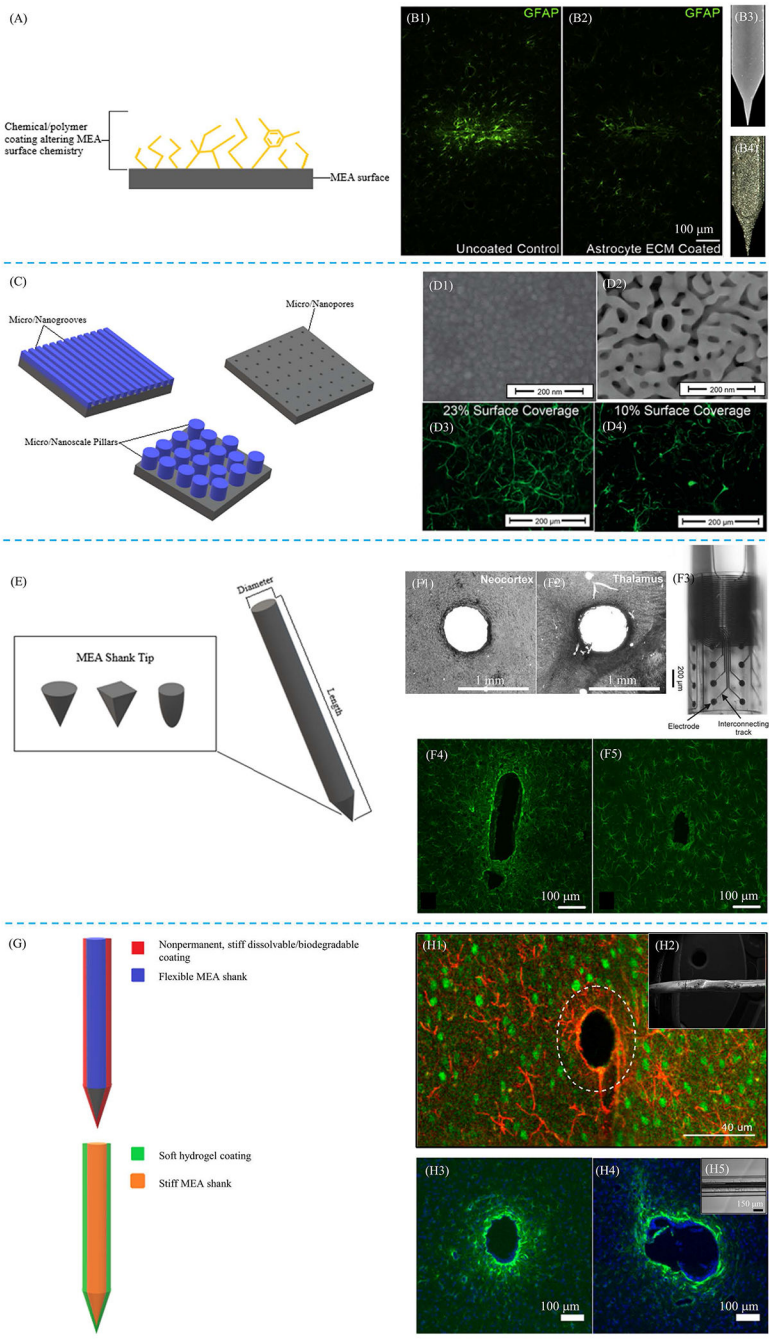

Figure 3:

Examples of MEA property modifications. Schematics demonstrating different types of surface modifications, including both surface chemistry (A) and topography (C), as well as modifications to surface geometry (E) and stiffness (G) are provided. (B1, B2) Glial fibrillary acidic protein (GFAP) stains comparing glial reactivity between an uncoated MEA (B1) with an MEA coated with astrocyte ECM (B2). The MEA coated with ECM showed reduced gliosis compared to uncoated MEA. (B3, B4) Surface images of uncoated MEA (B3) and astrocyte ECM coated MEA (B4). Reprinted from [61], Copyright 2018, with

permission from Elsevier. (D) Scanning electron microscopy (SEM) images of an unaltered MEA surface (D1) and MEA surface coated with nanoporous gold (D2). GFAP fluorescence images show reduced astrocytic coverage of nanoporous gold surface (D4), which had a 10% astrocytic coverage, compared to unaltered MEA surface (D3), which had a 23% astrocytic coverage. Reprinted (adapted) with permission from [74]. © 2015 American Chemical Society. (F1, F2) Histological GFAP staining of neural tissue with cylindrically shaped MEA implant, demonstrating limited tissue reaction resulting from the aforementioned applied geometry. (F3) Optical micrograph image of cylindrically shaped MEA implant. (F4, F5) GFAP stains comparing resulting gliosis between two different geometries, including floating (F4) and Michigan (F5) MEAs are also provided. Modified with permission and licensed under Creative Commons Attribution BY-NC-ND 4.0: © Biomed. Eng.-Biomed. Tech. [88]. Modified with permission and licensed under Creative Commons Attribution CC-BY 3.0: © Journal of Neural Engineering [89]. (H1) GFAP overlaid with neuronal nuclei (NeuN) demonstrating efficacy of using temporary MEA stiffening with dissolvable coatings for insertion into the brain. (H2) Electron micrograph image of dextran coating. (H3, H4) GFAP stains comparing an uncoated, stiff MEA (H3) with a stiff MEA coated with a 200 μm thick layer of soft, compliant hydrogel (H4). (H5) Image of soft hydrogel coating on MEA. Modified with permission and licensed under Creative Commons Attribution CC-BY 4.0. © Micromachines [97a]. Modified with permission and licensed under Creative Commons Attribution CC-BY 3.0 [97b]. Modified with permission and licensed under Creative Commons Attribution CC-BY 4.0. © Scientific Reports [102].

Table 1.

Strategies for improving microelectrode arrays

MEA Modifications	Surface Features/MEA Properties	Neural Cell Adhesion/Protein Adsorption	Neural Cell Grow/Loss	Foreign Body Response (FBR)	Signal Maintenance/MEA Longevity	References
Improving Surface Chemistry						
Natural materials						
Avitene™-MCH	White, cotton-like appearance; Collagen I, Collagen III, Collagen VI, and Lumican components	N/A	Large amounts of activated microglial growth; limited ramified microglial growth	No significant reduction in FBR compared to control	N/A	61
Neuroadhesive L1	Neuronal adhesion molecule	83% reduction in microglial adhesion; Good neuronal adhesion	Good neuroblast growth; limited neuronal cell death	Reduction in overall gliosis	N/A	64, 65a, 65b
Natural ECM	Vary depending on ECM coating type (i.e. astrocyte-derived coating: Collagen VI, Collagen XII, Tenascin N & W, Perlecan, Thromobospondin-1, Fetuin A)	Good neuronal cell adhesion	Limited neuronal cell death	Microglial suppression; reduction of astrogliosis	No significant electrode impedance following coat application	61, 62, 63
Sodium alginate	Na, C, N, and O surface chemistry; 400 μm thick coating	N/A	Limited neuronal cell death	Limited immunoreactivity	N/A	71
Synthetic materials						
Silica sol-gel	Smooth to rough texture, depending on composition (i.e. octyl, phenyl, aminopropyl, vinyl, glycidyl, octadecyl, thiol, isocyanate, chlorine, or iodine groups)	Good neuronal cell adhesion	Good neurite outgrowth; limited astrocyte growth	Limited FBR	N/A	66
PEDOT	Various different properties (i.e. fine textured porous surface with thin nanofilaments)	Reduced microglial adhesion	Limited neuronal cell death	Less severe FBR	Enhanced charge storage capacity and signal maintenance; enhanced noise and artifact reduction; PEDOT films increased MEA performance compared to controls during experimental period	67a, 67b, 67c
SOD Mimetic	MnTBAP-antioxidant coating	N/A	Limited cytotoxicity	Reduced microglial activity and superoxide radical production	Good shielding against reactive oxygen species	70
Nanomaterials/ Nanostructures	Carbon nanotubules on platinum cochlear neural electrodes	Stable cell adhesion	Stable cell growth	N/A	Decreased impedance and increased capacitance	69
	Polypyrrol nanotubes augmented with gold nanoparticles	N/A	No significant cytotoxicity	N/A	Tenfold decrease in electrochemical impedance	68

MEA Modifications	Surface Features/MEA Properties	Neural Cell Adhesion/Protein Adsorption	Neural Cell Grow/Loss	Foreign Body Response (FBR)	Signal Maintenance/MEA Longevity	References
Improving Surface Topography						
Parallel nano/micro groves	Nanopatterned parallel grooves 200 nm wide, 200nm deep, and 300 nm spacing	No significant difference in cell adhesion	Larger neuronal density at 4 weeks post implantation compared to control	No significant reduction of neuroinflammation	Nanopatterned groves did not degrade during study period	77
Nano/micro pillars	Microscale pillars with interspacings of 6-8 μm	Inhibition of platelet adsorption	N/A	N/A	N/A	59a
	580-800 nm long, 150-200 nm diameter nanopillars	Decent neural cell adhesion	More stable neural cell density compared to other tested topographies	No significant difference to control or other implants	N/A	78
Nano/micro pores	Nanoporous gold surface	Increased neuronal cell coverage, decreased astrocytic coverage	Good neural cell growth	Reduced glial scar formation	Might enhance neuron-electrode coupling	74
Improving Surface Geometry						
Smaller MEAs	15 μm Michigan electrodes and microwire electrodes	N/A	Lower neuronal cell loss compared to larger electrodes	Less severe FBR compared to larger electrodes	Microwire electrodes had better signal-to-noise ratio; No significant effect of size on electrode performance	87
Cylindrical shank	Polyamide cylindrically shaped depth probes	N/A	Neuronal death minimal around probe; moderate cell death in neocortex 25 μm from probe	Weak to moderate FBR around shank	Reduction in signal-to-noise ratio over the course of 9 weeks; Stable MEA recording activity for several weeks	88
Floating MEAs	Silicon wafer dummy floating electrodes coated with hexamethyldisilazane, photoresist, and Parylene-C	N/A	N/A	More significant FBR when implanted in spinal cord compared to brain; microglial reactivity did not increase over time	N/A	89
Stiffness Modifications for MEAs						
Flexible/soft MEAs	Parylene-C sinusoidal MEAs	N/A	Increase in neuronal cell density near probe	Significantly reduced astrocytic and microglial responses	N/A	92
	Ultraflexible nanoelectric thread	Seamless tissue integration	Normal astrocyte density and morphology; complete absence of neuronal degradation	Complete absence of glial scarring; no observable chronic tissue reaction	Persistently high signal-to-noise ratio; Stable recording performance for several months	93
	Ultrasoft MEAs composed of elastomers and conductive polymers	Reduced cell body distortion	Significantly higher neuronal cell density at 8 weeks compared to stiff implants	Significantly reduced FBR at 8 weeks	Successful acute nerve stimulation	95

MEA Modifications	Surface Features/MEA Properties	Neural Cell Adhesion/Protein Adsorption	Neural Cell Grow/Loss	Foreign Body Response (FBR)	Signal Maintenance/MEA Longevity	References
	Soft polypyrrol MEAs	Good MEA-substrate adhesion	N/A	N/A	High conductivity and successful recording of electrocorticograph signals; rat ischiadic nerve stimulation achieved	96
Temporarily stiff MEAs						
Stiff material coating	Flexible Parylene-C shank electrode with tapered profile; stiffened using applied dextran coating	Neuronal infiltration of dextran coat area following dissolution	No significant loss of neuronal cell density	Very limited glial scar tissue formation after 4 months	N/A	97a
	Flexible gold, Parylene-C insulated electrodes; stiffened using applied gelatin coating	N/A	N/A	N/A	Signal-to-noise ratio remained stable during 3-week period; MEA structure preserved during study period	98
Mechanical adaptivity	Poly(vinyl acetate)/tunicate cellulose nanocrystal nanocomposite MEAs	N/A	Significant neuronal cell loss initially, but neuronal cell recovery was seen over time 100 μm from implant	Significantly reduced FBR long-term at 2, 6, and 18 weeks	Stable electrochemical impedance spectra for 16 weeks	94b, 100
Stiff MEAs with surface modifications	Stiff glass capillary neural probes coated with soft PEG-DMA hydrogel	N/A	N/A	Significant reduction in glial scarring	N/A	102